



## Short Communication

## Efficient organic solar cells achieved at a low energy loss

Wenrui Liu<sup>a,b,1</sup>, Jianyun Zhang<sup>a,b,1</sup>, Shengjie Xu<sup>a,b,\*</sup>, Xiaozhang Zhu<sup>a,b,\*</sup><sup>a</sup> Beijing National Laboratory for Molecular Sciences, CAS Key Laboratory of Organic Solids, Institute of Chemistry, Chinese Academy of Sciences, Beijing 100190, China<sup>b</sup> School of Chemical Sciences, University of Chinese Academy of Sciences, Beijing 100190, China

## ARTICLE INFO

## Article history:

Received 28 June 2019

Received in revised form 1 July 2019

Accepted 3 July 2019

Available online 5 July 2019

© 2019 Science China Press. Published by Elsevier B.V. and Science China Press. All rights reserved.

Organic photovoltaics (OPVs) have attracted much attention because of the advantages in low-cost and large-area fabrication and the great potentials in achieving flexible and semi-transparent devices [1]. However, compared with inorganic and perovskite solar cells [2], OPVs show relatively low photoelectric conversion efficiencies, which is admittedly attributed to intrinsically low dielectric constants of organic materials [3] resulting in large energy losses ( $E_{\text{loss}} = E_g - qV_{\text{oc}}$ , where  $E_g$  is the optical bandgap of the photoactive layer,  $V_{\text{oc}}$  is the open-circuit voltage of photovoltaic devices and  $q$  is elementary charge). For the traditional bulk-heterojunction OPVs applying fullerene derivatives as the electron acceptors, the  $E_{\text{loss}}$ s are always higher than 0.6 eV, which limits the power conversion efficiencies (PCEs) less than 12% [4]. With the rapid development of fused-ring electron acceptors especially with an acceptor (A)-donor (D)-acceptor (A) arrangement [5], PCEs of OPV devices quickly surpassed 12% and even reached 16% in a very short period [6–10], in quite a few of which the  $E_{\text{loss}}$ s are less than 0.6 eV.

Although it is common for inorganic or perovskite solar cells, high-performance OPVs with the  $E_{\text{loss}}$ s less than 0.5 eV are quite rare up to date, which means that the  $E_{\text{loss}}$  is still the key factor that limits the photovoltaic efficiency of the OPV technique. Nonetheless, progresses in the development of efficient OPVs by reducing the  $E_{\text{loss}}$  to less than 0.5 eV have been made in the past few years. Xu et al. [11] designed and synthesized a large-bandgap polymer donor PBDBT-TDZ, which is based on the electron-rich benzo[1,2-*b*:4,5-*b'*]dithiophene and electron-deficient 1,3,4-thiadiazole moieties. By combining a representative non-fullerene acceptor, ITIC, the PBDBT-TDZ-based devices delivered a maximum PCE ( $\text{PCE}_{\text{max}}$ ) of 12.8% with a small  $E_{\text{loss}}$  of 0.48 eV. By introducing a highly elec-

tron-rich core, dithienopicenocarbazole, Yao et al. [12] developed an electron acceptor DTPC-DFIC that shows an absorption onset at 1,021 nm in thin film, which corresponds to a small optical bandgap of 1.21 eV. By using the low-bandgap polymer PTB7-Th as the electron donor, DTPC-DFIC-based devices showed a  $\text{PCE}_{\text{max}}$  of 10.21% with an extremely low  $E_{\text{loss}}$  of 0.45 eV. In our previous work, we developed a large-bandgap polymer donor BBTA by introducing the weakly electron-accepting benzo[1,2-*d*:4,5-*d'*]bisthiazole [13]. By matching with a low-bandgap electron acceptor ZITI-Br, a  $\text{PCE}_{\text{max}}$  of 11.08% was achieved with a small  $E_{\text{loss}}$  of 0.50 eV. Quite recently, Yuan et al. [14] developed an efficient electron acceptor Y6 that shows an absorption onset at 931 nm leading to an optical bandgap of 1.33 eV. Y6-based devices showed a very high  $\text{PCE}_{\text{max}}$  of 15.7% with a low  $E_{\text{loss}}$  of ca. 0.50 eV.

By enhancing the quinoidal resonance of donor-acceptor systems, we are recently focused on the design of molecular acceptors (ATT) [15] that have been successfully applied in binary, ternary, semi-transparent and tandem solar cells [16]. In those examples, the thieno[3,4-*b*]thiophene (TT) moiety with the unique quinoid-resonance effect is utilized to link the electron-rich and -deficient moieties by four  $\sigma$ -bonds, forming an A-Q-D-Q-A arrangement (Fig. S1a online). Quinoxaline (Qx) [17] is similar to TT in terms of its quinoid-resonance effect and is widely applied for the design of polymer donors. By fusing Qx into the heteroarene cores (Fig. S1b online), we can anticipate a decreased reorganization energy deriving from reduced free  $\sigma$ -bonds in the target molecular acceptor, which may facilitate electron transport and intermolecular packing. With that idea in mind, we report herein the design and synthesis of an electron acceptor AQx with a new quinoxaline-containing fused core (Fig. 1a) that shows a high molar absorption coefficient of  $1.93 \times 10^5 \text{ L mol}^{-1} \text{ cm}^{-1}$  and a narrow optical bandgap of 1.35 eV. By matching with a middle-bandgap polymer donor PBDB-TF, high PCEs of up to 13.31% are obtained at an  $E_{\text{loss}}$  as small as 0.45 eV that is, to the best of our knowledge,

\* Corresponding authors.

E-mail addresses: [xushengjie@icc.ac.cn](mailto:xushengjie@icc.ac.cn) (S. Xu), [xzzhu@icc.ac.cn](mailto:xzzhu@icc.ac.cn) (X. Zhu).<sup>1</sup> These authors contributed equally to this work.

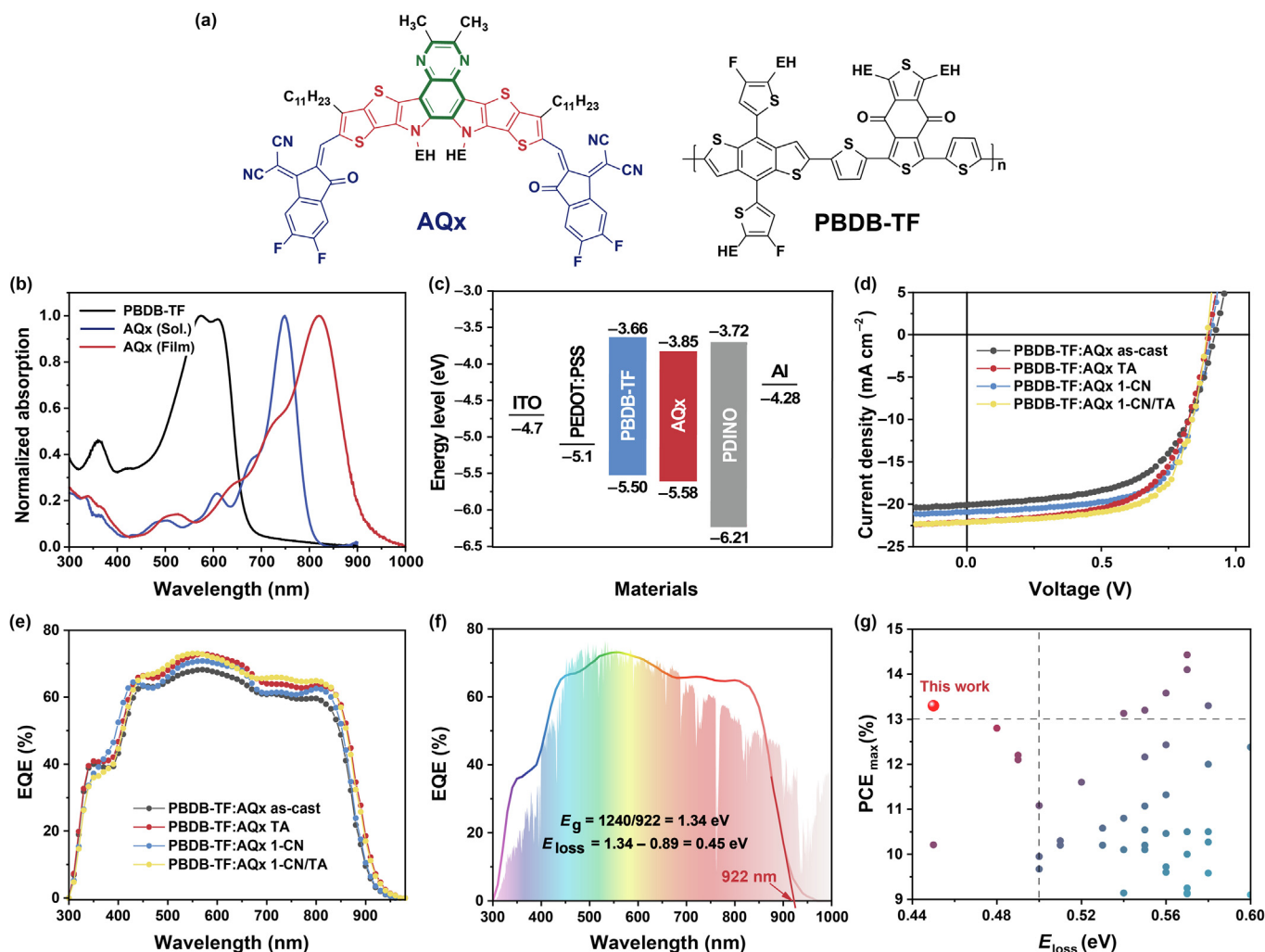


**Fig. 1.** Materials, photoelectric property and photovoltaic performance. (a) Molecular structures of AQx and PBDB-TF. (b) UV-vis-NIR absorption spectra. (c) Energy diagram of materials used in OPV devices. (d) Characteristic *J-V* curves of AQx-based OPVs under AM 1.5 G irradiation (100 mW cm<sup>-2</sup>). (e) The corresponding EQE curves. (f) The method for the determination of  $E_{loss}$  with the photon flux spectrum of solar radiation as the background. (g) Binary OPVs with the PCE<sub>max</sub> over 9% and  $E_{loss}$  below 0.6 eV reported in literatures.

the smallest value for the binary OPVs with PCEs over 13% reported to date [18].

AQx is synthesized from dialdehyde 13,14-bis(2-ethylhexyl)-6,7-dimethyl-3,10-diundecyl-13,14-dihydrothieno[2'',3':4,5']thieno[2',3':4,5]pyrrolo[3,2-f]thieno[2'',3':4,5']thieno[2',3':4,5]pyrrolo[2,3-h]quinoxaline-2,11-dicarbaldehyde and 2-(5,6-difluoro-3-oxo-2,3-dihydro-1*H*-inden-1-ylidene)malononitrile by the Knoevenagel condensation reaction and is fully characterized by the conventional NMR and mass analyses as shown in the [Supplementary data](#). AQx possesses a good solution processability because of its high solubility in common organic solvents such as chloroform, chlorobenzene, toluene and etc. The thermostability is determined by the thermogravimetric analysis as shown in [Fig. S2](#) (online), which indicates a high decomposition temperature of up to 347 °C at a 5 wt%. The normalized absorption spectra of AQx in solution and thin film are shown in [Fig. 1b](#). AQx exhibits a maximum absorption peak at 749 nm with a high molar absorption coefficient of  $1.93 \times 10^5$  L mol<sup>-1</sup> cm<sup>-1</sup> in chloroform, which is significantly red-shifted to 820 nm in thin film. Moreover, the broader absorption is observed ranging from 500 to 950 nm, which is complementary to that of PBDB-TF. The optical bandgap of AQx is estimated to be 1.35 eV according to the absorption onset in thin film,

918 nm. Cyclic voltammetry was performed to evaluate the frontier orbital energy levels of AQx. As shown in [Fig. 1c](#), the highest occupied molecular orbital (HOMO) and the lowest unoccupied molecular orbital (LUMO) energy levels of AQx are -5.58 and -3.85 eV, respectively. The HOMO offset between PBDB-TF and AQx is small, 0.08 eV, which is often observed for the state-of-the-art non-fullerene OPVs with a materials combination of a large/middle-bandgap donor and a low-bandgap acceptor and may bring a small energy loss.

To investigate the photovoltaic performance of AQx, we fabricated OPV devices with a conventional configuration of indium tin oxide (ITO)/poly(3,4-ethylenedioxythiophene):poly(styrenesulfonate) (PEDOT:PSS)/active layer/3,3'-(1,3,8,10-tetraoxoanthra[2,1,9-*def*:6,5,10-*d'**ef'*]diisoquinoline-2,9(1*H*,3*H*,8*H*,10*H*)-diyl)bis(*N,N*-dimethylpropan-1-amine oxide) (PDINO)/Al, where AQx and PBDB-TF were applied as the electron acceptor and donor materials, respectively. Originally, the as-cast devices exhibit the PCE<sub>max</sub> of up to 10.99%. To further improve the photovoltaic performance, the device optimization based on thermal annealing (TA), solvent additives and active layer thickness were systematically performed with the detailed photovoltaic parameters being listed in [Tables S1–S3](#) (online). A combination of 0.25 v/v% of 1-chloronaphthalene

(1-CN) as the solvent additive and thermal annealing at 100 °C for 10 min was used to tune the morphology of the active layer. The optimized **AQx**-based device shows a much improved short-circuit current ( $J_{sc}$ ) from 20.06 to 22.18 mA cm<sup>-2</sup> and fill factor (FF) from 59.34% to 67.14% with a comparable  $V_{oc}$  of 0.893 V, delivering the highest PCE<sub>max</sub> of 13.31%. The corresponding current density-voltage ( $J$ - $V$ ) and the external quantum efficiency (EQE) curves are shown in Fig. 1d and e. The **AQx**-based device shows a broad and high EQE response in the 300–900 nm region, which is consistent with the absorption spectra of the corresponding photoactive components and matches well with the photon flux spectrum of solar radiation (Fig. 1f). The calculated  $J_{sc}$ s based on the integration of the EQE spectra at different conditions are in good agreement with those obtained from the  $J$ - $V$  curves with minor errors of 2%–3%. We calculated the  $E_{loss}$ s of **AQx**-based devices according to the equation:  $E_{loss} = E_g - qV_{oc}$ , in which  $E_g$  is determined based on the EQE spectra. All the  $E_{loss}$ s of the blend films processed at different conditions are well below 0.47 eV and reach 0.45 eV for the most optimized device (Table S1 online).

We investigated the relationship between the device performance and optimization conditions. According to the analysis on the charge transport property examined by the space-charge-limited-current method (Fig. S4 online), the improved FF and  $J_{sc}$  in the most optimized device can be attributed to the higher charge carrier mobilities ( $\mu_h$ :  $2.06 \times 10^{-4}$  vs.  $1.50 \times 10^{-4}$  cm<sup>2</sup> V<sup>-1</sup> s<sup>-1</sup>;  $\mu_e$ :  $2.10 \times 10^{-4}$  vs.  $1.84 \times 10^{-4}$  cm<sup>2</sup> V<sup>-1</sup> s<sup>-1</sup>) and the more balanced  $\mu_h/\mu_e$  of approaching 1, which is summarized in Table S1 (online). We measured the variation of the photocurrent density ( $J_{ph}$ ) versus the effective voltage ( $V_{eff}$ ) to examine the efficiency of exciton dissociation and extraction property. As shown in Fig. S5a (online), the  $J_{ph}$  reaches saturation at a high  $V_{eff}$  of 2 V. The ratios of  $J_{ph}/J_{sat}$  at the four conditions are 90.66% (as-cast), 93.94% (TA), 94.58% (1-CN) and 95.52% (TA + 1-CN), respectively. Compared with the former three devices, the most optimized blend film shows the highest exciton dissociation probability, agreeing well with the best photovoltaic performance. We examined the charge recombination process by measuring the  $J_{sc}$  versus  $P_{light}^\alpha$ .  $\alpha$  is estimated from the formula:  $J_{sc} \propto P_{light}^\alpha$  as shown in Fig. S5b (online). The  $\alpha$  values are similar for the as-cast and post-treated devices, 0.95–0.96, which implies that those device treatments do not affect recombination process and suggests the negligible bimolecular recombination.

The surface morphology of PBDB-TF:**AQx** blend films is investigated by the atomic force microscopy (AFM) as shown in Fig. S6a (online). The root-mean-square (RMS) roughness of the as-cast blend film is estimated to be 0.77 nm, which means an excellent miscibility of PBDB-TF and **AQx**. After addition of 0.25 v/v% 1-CN or thermal annealing, RMS values are slightly increased, implying enhanced aggregation. The most optimized blend shows a RMS roughness of 1.44 nm, which is moderate and is beneficial for charge transport. Moreover, we applied transmission electron microscopy (TEM) to investigate the bulk morphology. As shown in the TEM images (Fig. S6b online), larger phase separation can be observed in the as-cast blend while and in the optimized blends, nanoscale fibrillar interpenetrating network is presented, which is favorable for charge dissociation and transport.

In conclusion, a new molecular acceptor **AQx** was designed and synthesized by fusing the quinoxaline moiety with the quinoid-resonance effect to the D-A system. **AQx** exhibits a very low optical bandgap of 1.35 eV in thin film. By matching with a middle-bandgap polymer donor PBDB-TF, **AQx**-based devices show high PCEs of up to 13.31% with careful optimizations. Noteworthy, **AQx**-based OPVs exhibit  $E_{loss}$ s of low to 0.45 eV, the smallest value for the binary OPVs with PCEs over 13% reported so far, which is shown in

Fig. 1g and Table S4 (online). The investigation on the origin of such a small  $E_{loss}$  is in progress in our group and will be reported in due course.

### Conflict of interest

The authors declare that they have no conflict of interest.

### Acknowledgments

This work was financially supported by the National Key R&D Program of China (2017YFA0204700), the Strategic Priority Research Program of the Chinese Academy of Sciences (XDB12010200) and the National Natural Science Foundation of China (21572234, 21661132006, 91833304, 21805289).

### Author contributions

Xiaozhang Zhu conceived and directed the project. Wenrui Liu and Shengjie Xu synthesized **AQx**. Jianyun Zhang performed the device fabrication and characterization.

### Appendix A. Supplementary data

Supplementary data to this article can be found online at <https://doi.org/10.1016/j.scib.2019.07.005>.

### References

- [1] Krebs FC, Espinosa N, Hösel M, et al. 25<sup>th</sup> anniversary article: rise to power – OPV-based solar parks. *Adv Mater* 2014;26:29–39.
- [2] Yao J, Thomas K, Michelle S, et al. Quantifying losses in open-circuit voltage in solution-processable solar cells. *Phys Rev Appl* 2015;4:014020.
- [3] Chen S, Tsang S-W, Lai T-H, et al. Dielectric effect on the photovoltage loss in organic photovoltaic cells. *Adv Mater* 2014;26:6125–31.
- [4] Zhao J, Li Y, Yang G, et al. Efficient organic solar cells processed from hydrocarbon solvents. *Nat Energy* 2016;1:15027.
- [5] Yan C, Barlow S, Wang Z, et al. Non-fullerene acceptors for organic solar cells. *Nat Mater* 2018;3:18003.
- [6] Xiao Z, Jia X, Li D, et al. 26 mA cm<sup>-2</sup>  $J_{sc}$  from organic solar cells with a low-bandgap nonfullerene acceptor. *Sci Bull* 2017;62:1494–6.
- [7] Xiao Z, Jia X, Ding L. Ternary organic solar cells offer 14% power conversion efficiency. *Sci Bull* 2017;62:1562–4.
- [8] Liu L, Liu Q, Xiao Z, et al. Induced J-aggregation in acceptor alloy enhances photocurrent. *Sci Bull* 2019;64:1083–6.
- [9] Meng L, Zhang Y, Wan X, et al. Organic and solution-processed tandem solar cells with 17.3% efficiency. *Science* 2018;361:1094–8.
- [10] Fan B, Zhang D, Li M, et al. Achieving over 16% efficiency for single-junction organic solar cells. *Sci China Chem* 2019;62:746–52.
- [11] Xu X, Yu T, Bi Z, et al. Realizing over 13% efficiency in green-solvent-processed nonfullerene organic solar cells enabled by 1,3,4-thiadiazole-based wide-bandgap copolymers. *Adv Mater* 2018;30:1703973.
- [12] Yao Z, Liao X, Gao K, et al. Dithienopyrenocarbazole-based acceptors for efficient organic solar cells with optoelectronic response over 1,000 nm and an extremely low energy loss. *J Am Chem Soc* 2018;140:2054–7.
- [13] Chen N-Y, Yue Q, Liu W, et al. A benzo[1,2-d:4,5-d']bisthiazole-based wide-bandgap copolymer semiconductor for efficient fullerene-free organic solar cells with a small energy loss of 0.50 eV. *J Mater Chem A* 2019;7:5234–8.
- [14] Yuan J, Zhang Y, Zhou L, et al. Single-junction organic solar cell with over 15% efficiency using fused-ring acceptor with electron-deficient core. *Joule* 2019;3:1140–51.
- [15] Liu F, Zhou Z, Zhang C, et al. A thieno[3,4-b]thiophene-based non-fullerene electron acceptor for high-performance bulk-heterojunction organic solar cells. *J Am Chem Soc* 2016;138:15523–6.
- [16] Zhou Z, Xu S, Song J, et al. High-efficiency small-molecule ternary solar cells with a hierarchical morphology enabled by synergizing fullerene and non-fullerene acceptors. *Nat Energy* 2018;3:952–9.
- [17] Desta G, Mario P, Margherita B, et al. Recent development of quinoxaline based polymers/small molecules for organic photovoltaics. *Adv Energy Mater* 2017;7:1700575.
- [18] Zou Y, Dong Y, Sun C, et al. High-performance polymer solar cells with minimal energy loss. *Chem Mater* 2018;31:4222–7.



Wenrui Liu obtained her B.S. degree from Shaanxi Normal University in 2016. Now, she is a Ph.D. student in Institute of Chemistry, Chinese Academy of Sciences (ICCAS) under the supervision of Prof. Xiaozhang Zhu. Her work focuses on the design and synthesis of new electron acceptors for organic solar cells.



Xiaozhang Zhu got his Ph.D. degree from Institute of Chemistry, Chinese Academy of Sciences in 2006, which was followed by postdoctoral research at Ulm University and University of Tokyo as an Alexander von Humboldt Fellow and JSPS Fellow, respectively. In 2012, he joined ICCAS as a full professor. Currently, his research interests include organic optoelectronic materials and their applications in organic solar cells and organic thermoelectrics.



Shengjie Xu received his Ph.D. degree from ICCAS in 2017 under the supervision of Prof. Xiaozhang Zhu. He is currently an assistant professor at CAS Key Laboratory of Organic Solids, ICCAS. He is focused on the development of new photovoltaic materials.